UV Photoelectron Spectra of the μ-Hydrido Bridge-Bonded Molecules B_2H_6, $GaBH_6$, and Ga_2H_6

John M. Dyke,* Darren Haggerston, and Oliver Warschkow

Department of Chemistry, University of Southampton, Southampton SO17 1BJ, U.K.

Lester Andrews, Anthony J. Downs, and Philip F. Souter

Inorganic Chemistry, University of Oxford, Oxford OX1 3QR, U.K.

Received: October 13, 1995; In Final Form: November 6, 1995[⊗]

The He I UV photoelectron spectra of both digallane, Ga_2H_6, and gallaborane, $GaBH_6$, have been recorded for the first time, affording ionization energies in good agreement with calculated values. Comparisons are made between the photoelectron spectra of Ga_2H_6, $GaBH_6$, and the previously studied B_2H_6. One band for each molecule is sufficiently well-resolved to reveal a vibrational progression in one or more totally symmetric $M-H_t$ stretching modes (M = Ga or B; t = terminal) of the molecular ion: this assignment is confirmed for digallane by studies on Ga_2D_6.

Introduction

The bridge-bonded molecule digallane, $H_2Ga(\mu\text{-}H)_2GaH_2$, has been identified largely on the basis of the infrared and Raman spectra of the gaseous and matrix-isolated species[1−5] and by the electron-diffraction pattern of the free molecule.[2] *Ab initio* and density functional calculations have predicted a D_{2h} minimum energy structure for the molecule and vibrational properties in good agreement with the observed infrared and Raman spectra.[6−13] Similar calculations give grounds for believing that the aluminum analogue Al_2H_6 is more stable than Ga_2H_6 with respect to its elements, but Al_2H_6 has yet to be authenticated in practice by anything more compelling than a molecular ion peak in the mass spectrum of the vapors formed when aluminum is evaporated into a hydrogen atmosphere.[14] By contrast, the familiar diborane molecule, B_2H_6, is well-known to possess a bridged, dimeric D_{2h} structure on the evidence of extensive computational[8−13,15−19] and experimental[20−33] investigations of this molecule stretching back over 50 years. The "intermediate" molecule gallaborane, $GaBH_6$, has been identified by its vibrational spectra[24] and electron-diffraction pattern[35] as having the structure $H_2Ga(\mu\text{-}H)_2BH_2$, again with properties close to those anticipated by theoretical studies.[36,37]

Additional spectroscopic investigations on digallane and gallaborane are desirable for characterizing more fully these μ-hydrido bridge-bonded species. This work reports a He I photoelectron spectroscopic study of these molecules designed to probe their electronic structure and bonding. Diborane has previously been the subject of extensive studies by photoelectron spectroscopy (PES);[24−27] it is of much interest therefore to compare the photoelectron spectrum of diborane with those displayed by digallane and gallaborane.

Experimental Section

All UV photoelectron spectra were recorded on a single detector photoelectron spectrometer specifically designed for the study of short-lived molecules, which has been described previously.[38−40] Most experiments were performed with a He I (21.22 eV) photon source, although some were performed with He II (40.81 eV) radiation.

Gallaborane and digallane were synthesized by the reactions between monochlorogallane, $[H_2GaCl]_2$, and $LiXH_4$ (X = B, Ga, respectively) described previously.[2,4,34,35] The perdeuteriated version of digallane was prepared in an analogous manner from $[D_2GaCl]_2$ and $LiGaD_4$. These compounds are highly reactive and thermally fragile, requiring the reaction to be carried out in an all-glass apparatus.[2,4] The relevant purpose-built apparatus was rigorously conditioned by "flaming out" under continuous pumping so as to remove any residual moisture or other volatile impurities adsorbed on the inner walls. The glass ampule containing the purified sample was attached to a specially constructed glass inlet system *via* a break-seal. The assembly consisted of a jacketed, single-sleeved tube similar to that described in ref 3. The inner nozzle of the tube was maintained at *ca.* −30 °C by directing cold nitrogen gas over it, thereby minimizing decomposition of the vapor sample. In each experiment the ampule containing the sample was held at −196 °C until the break-seal had been opened. The ampule was allowed to warm slowly until a photoelectron spectrum of the vapor could be recorded. The most intense spectra were observed with sample temperatures of −45 and −23 °C for gallaborane and digallane, respectively.

Diborane was prepared from the reaction of $NaBH_4$ with concentrated H_2SO_4.[41] As B_2H_6 is much more robust than either $GaBH_6$ or Ga_2H_6, it could be stored at room temperature in a glass bulb equipped with a Young's greaseless valve. The bulb was attached to the inlet system and the vapor introduced into the spectrometer *via* a needle valve without the need for any cooling of the glassware. The He I signal achieved with diborane was sufficiently intense and long-lived to encourage the higher energy He II photoelectron spectrum to be measured. This was accomplished by reducing the pressure of helium in the discharge lamp to 0.1 Torr and increasing the current from 55 to 210 mA; He II photons then constituted approximately 10% of the lamp output. Attempts were also made to obtain the He II photoelectron spectra of gallaborane and digallane, but these met with little success.

In each experiment, spectral calibration was effected using the first He I α bands of methyl iodide and argon and the typical experimental resolution, as measured for the argon 3p doublet, was *ca.* 30 meV.

[⊗] Abstract published in *Advance ACS Abstracts,* January 1, 1996.

0022-3654/96/20100-2998$12.00/0

TABLE 1: Calculated and Experimental Geometrical Parameters of Molecules of the Type $H_2M(\mu\text{-}H)_2M'H_2$ (M, M′ = B or Ga)

	M = B, M′ = B		M = B, M′ = Ga		M = Ga, M′ = Ga	
parameter	calcd[e]	expt[a]	calcd[e]	expt[b]	calcd[e]	expt[c]
r(M−M′)/Å	1.793	1.743	2.229	2.179	2.650	2.580
r(M−H_t)/Å	1.188	1.184	1.193	1.234	1.561	1.519
r(M−H_b)/Å	1.329	1.314	1.305	1.334	1.775	1.710
r(M′−H_t)/Å	1.188	1.184	1.559	1.586	1.561	1.519
r(M′−H_b)/Å	1.329	1.314	1.784	1.826	1.775	1.710
∠H_t−M−H_t/deg	122.4	121.5	121.2	120[d]	128.9	130.0
∠H_b−M−H_b/deg	95.2	96.9	106.3	113.4	83.4	82.1
∠H_t−M′−H_t/deg	122.4	121.5	128.8	145[d]	128.9	130.0
∠H_b−M′−H_b/deg	95.2	96.9	71.7	75.3	83.4	82.1

[a] Equilibrium r_e structure parameters taken from ref 30. [b] r_a structure parameters taken from ref 35. [c] r_a structure parameters taken from ref 2. [d] Parameter fixed at this value in the analysis of the electron-diffraction pattern. [e] Calculated values in this work; see text for further details.

Computational Details

All experiments were supplemented by *ab initio* molecular orbital calculations. Gaussian basis sets were used, and these were constructed as follows.

For boron, Huzinaga's (9s5p) basis set[42] was contracted to approximately double ζ (DZ) quality following the method of Dunning[43] and augmented by a single d function (exponent 0.37).[44] The hydrogen basis set used was Dunning's DZ contraction[43] of the (4s) basis of Huzinaga,[42] augmented by a p function (exponent 0.75).[8] Finally, for gallium, the (14s11p5d) basis of Dunning[45] contracted to approximately DZ quality by Schaefer and Ma[46] was employed, supplemented by a d polarization function (exponent 0.21).[46]

Ab initio calculations were performed in this work on the ground state neutral molecule and all ionic states accessible by He I radiation. The self-consistent field (SCF) minimum energy geometries of ground state neutral B_2H_6, $GaBH_6$, and Ga_2H_6 were calculated *via* the method of analytic second derivatives, using the CADPAC 5.0 suite of programs[47] on the Convex C3840 at ULCC. The geometry of each molecule optimized to a μ-hydrido bridge-bonded structure, with D_{2h} symmetry in the cases of B_2H_6 and Ga_2H_6 and C_{2v} symmetry in the case of $GaBH_6$. The calculated molecular dimensions of B_2H_6, $GaBH_6$, and Ga_2H_6 are compared to experimental values, derived from gas-phase electron diffraction measurements.[2,30,35] in Table 1. Reasonably good agreement is evident, and these optimized geometries were used in subsequent *ab initio* calculations of vertical ionization energies (VIEs).

The valence orbital orderings were computed to be

$$...(2a_g)^2(2b_{1u})^2(1b_{2u})^2(1b_{3u})^2(3a_g)^2(1b_{2g})^2$$

$$...(9a_1)^2(10a_1)^2(4b_2)^2(4b_1)^2(11a_1)^2(5b_1)^2$$

$$...(8a_g)^2(8b_{1u})^2(4b_{2u})^2(4b_{3u})^2(9a_g)^2(4b_{2g})^2$$

for B_2H_6, $GaBH_6$, and Ga_2H_6, respectively.

For each molecule, the characteristics of related valence orbitals were found to be very similar on going from B_2H_6 to $GaBH_6$ to Ga_2H_6. For example, the $1b_{2g}$ orbital in B_2H_6, the $5b_1$ orbital in $GaBH_6$, and the $4b_{2g}$ orbital in Ga_2H_6 all consist of terminal H 1s contributions and contributions from the *n*p valence orbitals in the group 13 elements (n = 2, 4 for B, Ga). Taking Ga_2H_6 as an example, the four highest lying molecular orbitals ($4b_{2g}$, $9a_g$, $4b_{3u}$, and $4b_{2u}$) are all composed of linear combinations of Ga 4p and bridging and terminal H 1s atomic orbitals. The $8a_g$ and $8b_{1u}$ molecular orbitals are composed of Ga 4s and terminal H 1s contributions which interact in a bonding manner within each $-GaH_2$ terminal unit. The difference between the two molecular orbitals is that the coefficients of the contributing atomic orbitals were all positive in the lower $8a_g$ orbital, whereas in the $8b_{1u}$ orbital the coefficients of the H 1s and Ga 4s atomic orbitals are positive within one $-GaH_2$ terminal unit and negative within the other one.

TABLE 2: Computed Vertical Ionization Energies (eV) of B_2H_6 *via* Koopmans' Theorem, ΔSCF, and DFT Methods

orbital ionized	ionic state formed	KT[a]	ΔSCF[a]	ΔSCF + CISD[a]	ΔSCF + CISD + Q[a]	DFT[b]	expt[c]
$1b_{2g}$	X^2B_{2g}	12.81	12.39	12.29	12.19	11.44	11.88
$3a_g$	A^2A_g	13.98	13.30	13.34	13.28	12.75	13.35
$1b_{3u}$	B^2B_{3u}	14.59	14.21	14.03	13.89	13.02	13.93
$1b_{2u}$	C^2B_{2u}	14.91	13.88	14.42	14.48	14.97	14.76
$2b_{1u}$	D^2B_{1u}	17.35	16.93	16.53	16.31	14.89	16.08
$2a_g$	E^2A_g	23.90	*d*	*d*	*d*	20.93	21.42

[a] As stated in the text, the geometry used in these calculations was that derived from analytic second derivative calculations on $B_2H_6(X^1A_g)$. [b] As stated in the text, the geometry used in these calculations was the experimentally derived one.[30] [c] This work. [d] Problems were encountered with convergence of open-shell SCF calculations on this ionic state.

VIEs were calculated initially using Koopmans' theorem (KT)[48] applied to the SCF eigenvalues. In the case of diborane and digallane, the ΔSCF method was also used to account for electron reorganization on ionization. Electron correlation was also partially included by employing configuration interaction (CI) calculations, including single and double excitations (ΔSCF + CISD), on each state; allowance for the effect of quadruple excitations was made by invoking the Davidson approximation, Q.[49] All orbitals were included in the CI procedure, and all calculations were performed using the GAMESS ensemble of programs,[50] also on the Convex C3840 at ULCC. However, these calculations did not meet with complete success: it was found to be impossible to achieve convergence of the open-shell SCF calculation on the E^2A_g excited ionic state of either B_2H_6 or Ga_2H_6, despite resort to a variety of convergence aids. Some $GaBH_6$ excited ionic states were also expected to give convergence problems in view of the lower molecular symmetry. Accordingly, the decision was made to perform density functional (DFT) calculations on all three molecules and gain estimates of the VIEs *via* the transition state method. All DFT calculations were performed with the ADF program of Bearends *et al.*[51] on a Silicon Graphics Power Challenge workstation and employed the local density approximation with Slater's exchange and the VWN correlation functional.[52] The molecular geometries used were those determined from gas-phase electron diffraction studies.[2,19,31] All basis sets used were taken from the ADF basis set type V,[51] these being constructed as follows. For boron, a triple ζ plus one 3d and one 4f polarization function basis was employed, with a frozen core of 1s; the hydrogen basis set was of the same quality with one 2p and one 3d polarization function, and the gallium basis was of triple ζ quality augmented by one 4d and one 4f function, with orbitals up to 3p included in the frozen core.

Results

(a) Calculated Vertical Ionization Energies. The VIEs obtained from KT, ΔSCF, ΔSCF + CISD, and DFT calculations for diborane and digallane are shown in Table 2 and Table 4, respectively. Table 3 gives the VIEs for gallaborane calculated

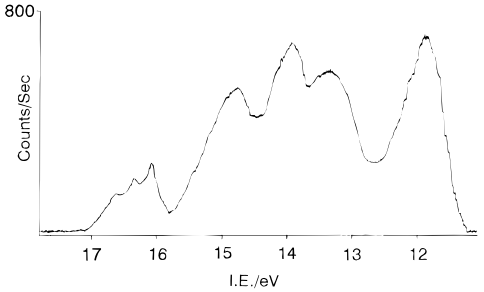

Figure 1. He I (21.22 eV) photoelectron spectrum of B_2H_6. Ordinate: counts/s. Abscissa: ionization energy/eV.

TABLE 3: Computed Vertical Ionization Energies (eV) of $GaBH_6$ *via* Koopmans' Theorem, ΔSCF, and DFT Methods

orbital ionized	ionic state formed	KT[a]	ΔSCF[a]	ΔSCF + CISD[a]	ΔSCF + CISD + Q[a]	DFT[b]	expt[c]
$5b_1$	X^2B_1	12.11	11.54	11.73	11.68	10.84	11.33
$11a_1$	A^2A_1	12.78	12.12	12.26	12.21	11.11	12.15
$4b_1$	B^2B_1	13.31	*d*	*d*	*d*	12.15	12.63
$4b_2$	C^2B_2	13.65	12.57	12.94	12.98	13.28	13.31
$10a_1$	D^2A_1	15.93	*d*	*d*	*d*	13.91	15.03
$9a_1$	E^2A_1	21.67	*d*	*d*	*d*	18.21	
$3b_1$	F^2B_1	33.29					

[a] As stated in the text, the molecular geometry used was that derived from analytic second derivative calculations on $GaBH_6(X^1A_1)$. [b] The molecular geometry used was the experimentally determined geometry.[35] [c] This work. [d] Problems were encountered with attempts at convergence of open-shell SCF calculations on this ionic state.

TABLE 4: Computed Vertical Ionization Energies (eV) of Ga_2H_6 *via* Koopmans' Theorem, ΔSCF, and DFT Methods

orbital ionized	ionic state formed	KT[a]	ΔSCF[a]	ΔSCF + CISD[a]	ΔSCF + CISD + Q[a]	DFT[b]	expt[c]
$4b_{2g}$	X^2B_{2g}	11.75	11.51	11.50	11.38	10.57	10.88
$9a_g$	A^2A_g	12.24	11.87	11.87	11.76	11.07	11.56
$4b_{3u}$	B^2B_{3u}	12.28	12.03	12.05	11.94	11.12	11.85
$4b_{2u}$	C^2B_{2u}	12.37	11.45	11.67	11.68	11.96	12.23
$8b_{1u}$	D^2B_{1u}	15.17	14.90	14.92	14.77	13.74	14.40
$8a_g$	E^2A_g	19.29	*d*	*d*	*d*	17.34	
$7b_{1u}$	F^2B_{1u}	32.77					

[a] As stated in the text, the molecular geometry used was that derived from analytic second derivative calculations on $Ga_2H_6(X^1A_g)$. [b] The geometry used in these calculations was the experimentally determined one.[2] [c] This work. [d] Problems were encountered with attempts at convergence of open-shell SCF calculations on this state.

by the KT and DFT methods. For each molecule, six ionic states are computed to be accessible by He I radiation.

(b) Experimental Results. (i) *B_2H_6*. The He I photoelectron spectrum recorded for diborane is shown in Figure 1. As can be seen from this figure, the spectrum contains four overlapping bands in the ionization energy range 11.0−15.5 eV with a separate, vibrationally resolved band at slightly higher ionization energy (*ca*. 16.0 eV). As the four bands at lower energy overlapped, it was possible to measure the adiabatic ionization energy (AIE) only for the first band. The VIEs were taken to be the band maxima measured from the spectrum.

The vibrationally resolved band is shown in expanded form in Figure 2a. Three vibrational components are clearly visible, with the adiabatic component being the most intense. Measurement of the separation of these components allowed $\bar{\omega}_e$ to be derived for this short vibrational progression. All the measured experimental ionization energies and the vibrational constant derived for the fifth band are shown in Table 5.

It was possible also to record the He II photoelectron spectrum of diborane, and this is shown in Figure 3. One extra band, at

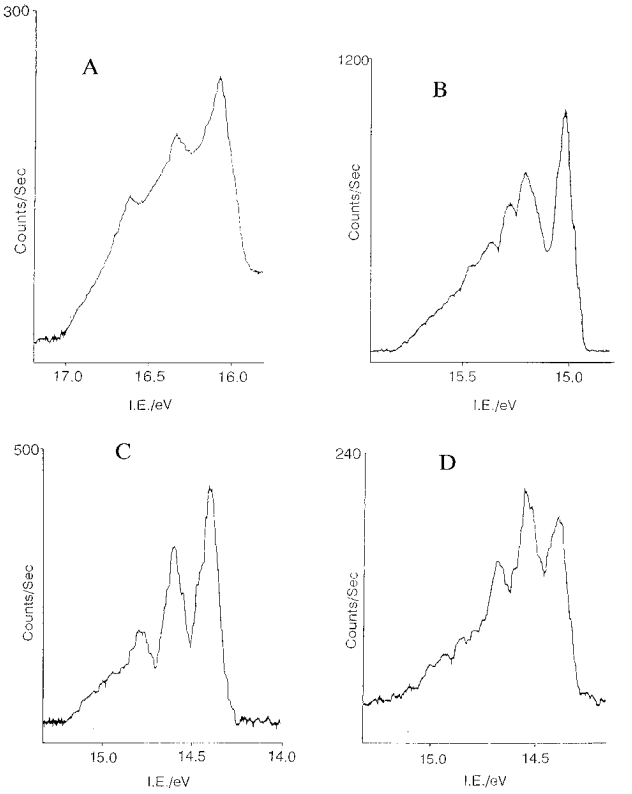

Figure 2. Expanded scan of the fifth bands in the He I photoelectron spectra of (A) B_2H_6, (B) $GaBH_6$, (C) Ga_2H_6, and (D) Ga_2D_6. In B, two vibrational progressions are present, as shown. Ordinate: counts/s. Abscissa: ionization energy/eV.

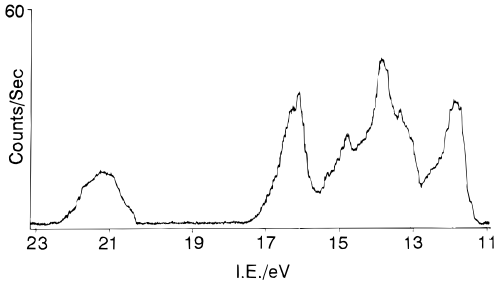

Figure 3. He II (40.81 eV) photoelectron spectrum of B_2H_6 recorded in the 11.0−23.0 eV ionization energy region. No other bands were observed at higher ionization energy. Ordinate: counts/s. Abscissa: ionization energy/eV.

TABLE 5: Experimental Ionization Energies (eV) and Vibrational Constant (cm^{-1}) Derived from the He I Photoelectron Spectrum of B_2H_6

orbital ionized[a]	AIE	VIE	$\bar{\omega}_e$
$1b_{2g}$	11.29 ± 0.01	11.88 ± 0.01	
$3a_g$		13.35 ± 0.03	
$1b_{3u}$		13.93 ± 0.02	
$1b_{2u}$		14.76 ± 0.01	
$2b_{1u}$	16.08 ± 0.01	16.08 ± 0.01	2178 ± 100
$2a_g$	20.50 ± 0.09	21.42 ± 0.09[b]	

[a] The full electronic configuration is $(1a_g)^2(1b_{1u})^2(2a_g)^2(2b_{1u})^2(1b_{2u})^2(1b_{3u})^2(3a_g)^2(1b_{2g})^2$. [b] This band was not observed in the He I photoelectron spectrum of B_2H_6 (see text); the quoted AIE and VIE values are taken from the He II spectrum.

21.42 eV, is observed as a result of using the higher energy photon source. The onset of this band occurs at 20.40 eV, an energy just within the range of He I radiation (21.22 eV). As the analyzer of the spectrometer used in the present studies discriminates against low-energy electrons, this sixth band is

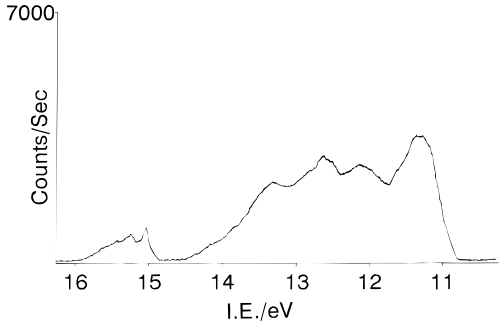

Figure 4. He I photoelectron spectrum of $GaBH_6$. Ordinate: counts/s. Abscissa: ionization energy/eV.

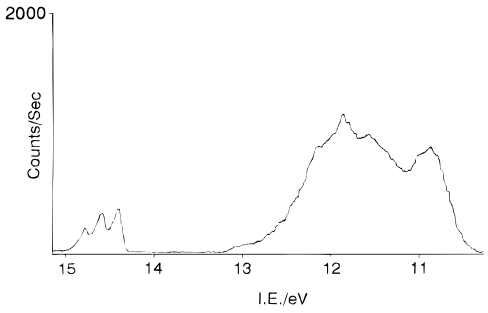

Figure 5. He I photoelectron spectrum of Ga_2H_6. Ordinate: counts/s. Abscissa: ionization energy/eV.

TABLE 6: Experimental Ionization Energies (eV) and Vibrational Constants (cm^{-1}) Derived from the He I Photoelectron Spectrum of $GaBH_6$

orbital ionized[a]	AIE	VIE	$\bar{\omega}_e(1)$	$\bar{\omega}_e(2)$
$5b_1$	10.80 ± 0.01	11.33 ± 0.01		
$11a_1$		12.15 ± 0.01		
$4b_1$		12.63 ± 0.01		
$4b_2$		13.31 ± 0.03		
$10a_1$	15.03 ± 0.01	15.03 ± 0.01	1480 ± 100[c]	1950 ± 100[c]
$9a_1$		*b*		

[a] The full electronic configuration is $(1a_1)^2(2a_1)^2(1b_2)^2(3a_1)^2(1b_1)^2(4a_1)^2(5a_1)^2(2b_2)^2(6a_1)^2(2b_1)^2(3b_2)^2(7a_1)^2(8a_1)^2(1a_2)^2(3b_1)^2(9a_1)^2(10a_1)^2(4b_2)^2(4b_1)^2(11a_1)^2(5b_1)^2$. [b] This band was not observed in the He I photoelectron spectrum of $GaBH_6$; no He II spectrum was obtained. [c] Two vibrational progressions are displayed by this band (see Figure 2b).

unlikely to be observed in the He I photoelectron spectrum. No bands to higher ionization energy could be detected.

(ii) $GaBH_6$. The He I photoelectron spectrum of gallaborane, illustrated in Figure 4, is very similar to that observed for diborane. Four overlapping bands are present in the ionization energy range 10.5−14.0 eV, with a single vibrationally resolved band at 15.03 eV VIE. As with diborane, it was possible to measure the AIEs only for the first and fifth bands. The VIEs were taken as the band maxima observed in the spectrum.

An expanded view of the fifth band is presented in Figure 2B. This feature is considerably more complex than the corresponding band of diborane as it consists of two vibrational progressions, each containing three components. The separation of these components can be used to calculate $\bar{\omega}_e$ for each progression. The experimentally determined AIEs, VIEs, and vibrational constants are presented in Table 6.

(iii) Ga_2H_6. Figure 5 displays the He I photoelectron spectrum of digallane. The similarity which the spectrum bears to those recorded for diborane and gallaborane is obvious: again, there are four overlapping bands, now in the ionization energy range 10.0−13.5 eV, plus a vibrationally resolved band approximately 1 eV higher in energy. No features to higher ionization energy could be detected with any certainty, although there may be a weak feature near 18 eV ionization energy, which was visible in some experiments but was too weak to be identified with any confidence. Once more, it was possible to measure the AIEs only for the first and fifth bands; the VIEs were taken as the positions of the observed band maxima.

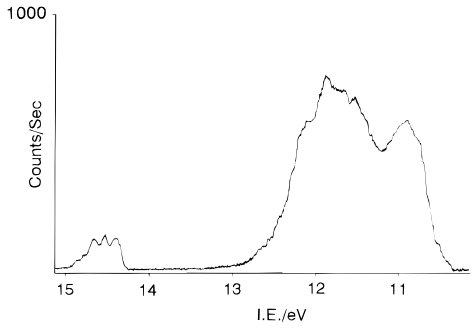

Figure 6. He I photoelectron spectrum of Ga_2D_6. Ordinate: counts/s. Abscissa: ionization energy/eV.

TABLE 7: Experimental Ionization Energies (eV) and Vibrational Constant (cm^{-1}) Derived from the He I Photoelectron Spectrum of Ga_2H_6

orbital ionized	AIE	VIE	$\bar{\omega}_e$
$4b_{2g}$	10.49 ± 0.01	10.88 ± 0.01	
$9a_g$		11.56 ± 0.03	
$4b_{3u}$		11.85 ± 0.03	
$4b_{2u}$		12.23 ± 0.03	
$8b_{1u}$	14.40 ± 0.01	14.40 ± 0.01	1540 ± 40
$8a_g$		—[b]	

[a] The full electronic configuration is $(1a_g)^2(1b_{1u})^2(2a_g)^2(2b_{1u})^2(1b_{2u})^2(1b_{3g})^2(3a_g)^2(3b_{1u})^2(1b_{3u})^2(1b_{2g})^2(4a_g)^2(4b_{1u})^2(2b_{2u})^2(2b_{3g})^2(5a_g)^2(5b_{1u})^2(2b_{3u})^2(2b_{2g})^2(3b_{2u})^2(6a_g)^2(3b_{3g})^2(6b_{1u})^2(7a_g)^2(3b_{3u})^2(1b_{1g})^2(1a_u)^2(3b_{2g})^2(7b_{1u})^2(8a_g)^2(8b_{1u})^2(4b_{2u})^2(4b_{3u})^2(9a_g)^2(4b_{2g})^2$. [b] This band was not seen with any confidence in the He I photoelectron spectrum of Ga_2H_6; no satisfactory He II spectrum could be obtained.

TABLE 8: Experimental Ionization Energies (eV) and Vibrational Constant (cm^{-1}) Derived from the He I Photoelectron Spectrum of Ga_2D_6

orbital ionized	AIE	VIE	$\bar{\omega}_e$
$4b_{2g}$	10.50 ± 0.01	10.90 ± 0.01	
$9a_g$		11.56 ± 0.02	
$4b_{3u}$		11.87 ± 0.03	
$4b_{2u}$		12.17 ± 0.03	
$8b_{1u}$	14.40 ± 0.01	14.54 ± 0.01	1135 ± 40
$8a_g$		*a*	

[a] This band was not seen with any confidence in the He I photoelectron spectrum of Ga_2D_6; no satisfactory He II spectrum could be obtained.

The vibrationally resolved fifth band is presented in more detail in Figure 2C. Three vibrational components are clearly observed, with the adiabatic component being the most intense. The vibrational constant derived for this progression is given in Table 7, along with the experimental vertical ionization energies of the five observed bands. Because the fifth band of Ga_2H_6 was clearly resolved and the He I spectrum was reasonably intense, it was thought worthwhile also to record the He I photoelectron spectrum of digallane-d_6, Ga_2D_6. This is shown in Figure 6. As expected, the overall spectral envelope in the ionization energy region 10.0−13.5 eV is very similar to that displayed by Ga_2H_6. The major difference is observed in the vibrational structure of the fifth band (Figure 2D). Once again, three members of a vibrational progression are observed, with the second component now the most intense. The value for $\bar{\omega}_e$ derived for this progression is quoted in Table 8 with the measured AIEs and VIEs.

Discussion

(i) B_2H_6. Several points emerge from a comparison of the calculated VIEs for B_2H_6 (Table 2) with the experimental values (Table 5). The KT VIEs are consistently too high, with the value for the C^2B_{2u} ionic state being in best agreement with experiment. The DFT values, on the other hand, are in general too low, but the best agreement with experiment is again provided by the C^2B_{2u} ionic state. All KT VIEs are lowered once electron reorganization is accounted for *via* the ΔSCF method. The $(1b_{2u})^{-1}$ ionization is predicted to be lower in energy than the $(1b_{3u})^{-1}$ ionization at the ΔSCF level, but KT predicts the reverse order. Taking into account the changes in electron correlation on ionization causes the ionic state ordering to revert to that predicted on the basis of Koopmans' theorem. In general, the ΔSCF + CISD + *Q* VIEs are in best agreement with experiment, with the same ionic state ordering as that predicted at the KT level of theory.

The ionic state ordering is therefore computed to be X^2B_{2g}, A^2A_g, B^2B_{3u}, C^2B_{2u}, D^2B_{1u}, and E^2A_g, in agreement with the conclusions of previous PES investigations.[25−27] The He I and He II photoelectron spectra recorded in this work (Figures 1 and 3) compare very favorably with those recorded earlier,[25−27] with the measured AIEs and VIEs being in good agreement. The value of $\bar{\omega}_e$ obtained for the vibrational progression observed in the D^2B_{1u} ionic state, 2180 ± 100 cm^{-1}, is close to that quoted in ref 26, *viz*., 2200 cm^{-1} (no error quoted). The $2b_{1u}$ orbital arises solely from a B 2s orbital bonding interaction with the terminal H 1s orbitals, with no contribution from the bridging H 1s orbitals. The form of this orbital suggests that the totally symmetric B−H_t stretching fundamental, ν_1, which possesses the value of 2524 cm^{-1} in the *neutral* molecule, will be excited on ionization. The authors in ref 26 also claimed to observe a vibrational progression in the first photoelectron band with a vibrational constant of 900 cm^{-1} (no error quoted). Unfortunately, it was not possible to resolve any vibrational structure in the first photoelectron band of B_2H_6 in this work.

A comparison of Figures 1 and 3 reveals the presence of an extra band in the He II spectrum associated with the $(2a_g)^{-1}$ ionization. Particularly interesting is the intensity change of the fifth band (the $(2b_{1u})^{-1}$ ionization), which increases in relation to the lower energy features in the spectrum on going from He I to He II radiation. Atomic subshell photoionization cross sections have been calculated by Yeh and Lindau for all elements $Z = 1-103$.[53] At the He I photon energy the B 2p and 2s cross sections are calculated as 1.934 and 1.716 Mb, respectively. However, at the He II photon energy the B 2p cross section drops considerably to 0.4227 Mb, whereas the B 2s cross section also drops, but to a much smaller extent, to 1.049 Mb. Hence, an ionization from a molecular orbital of B 2s and H 1s contributions is expected to gain intensity relative to ionizations from molecular orbitals which are composed of B 2p and H 1s contributions, on going from He I to He II radiation. Moreover, at He II photon energies the photoelectrons of the $(2b_{1u})^{-1}$ ionization possess much more kinetic energy than when He I radiation is used as the ionizing source. It follows that the discrimination of the analyzer against low-energy electrons will affect the band intensity of the $(2b_{1u})^{-1}$ ionization less in the He II spectrum. Both factors combine to give the observed intensity increase of the band associated with ionization to the D^2B_{1u} ionic state relative to the bands at lower ionization on going from He I to He II radiation.

(ii) $GaBH_6$. The He I photoelectron spectrum of $GaBH_6$ (Figure 4) is similar in overall spectral envelope to the B_2H_6 spectrum (Figure 1), albeit with several differences of detail. One such difference is that the first band is shifted by approximately 0.5 eV to lower energy. Secondly, the separation of the first and fourth band maxima is approximately 1 eV smaller than in B_2H_6. Finally, the fifth band is 1 eV lower in energy in $GaBH_6$ than in B_2H_6. These slight differences in the photoelectron spectra almost certainly reflect the Ga atom contribution to the valence molecular orbitals, as Ga possesses a lower first ionization energy than B.[54]

The only theoretical methods used that give VIEs for all ionic states in the He I energy range are the Koopmans' theorem and DFT calculations (Table 3). Once more, the KT VIEs are too high and the DFT VIEs too low in comparison with the experimental values. The ionic state ordering derived from each set of calculations is the same and correlates with the ionic state ordering in B_2H_6, taking into account the descent in symmetry. Furthermore, for each set of computed VIEs, the C^2B_2 ionic state KT value gives the best agreement with experiment, behavior analogous to that of diborane with due allowance for the change from D_{2h} to C_{2v} symmetry.

ΔSCF VIEs are available only for the X^2B_1, A^2A_1, and C^2B_2 ionic states as calculations for the other ionic states converged to the lowest energy state of appropriate symmetry. As a result, ΔSCF + CISD (+*Q*) calculations could be performed only on the X, A, and C ionic states. The results, which are included in Table 3, show that electron reorganization is greatest for the C^2B_2 ionic state. Again, this parallels the results obtained for B_2H_6, where the energy of the $^2B_{2u}$ ionic state is reduced by a sufficient amount to lower it below the $^2B_{3u}$ ionic state at the ΔSCF level. The ΔSCF + CISD calculations raise the VIE of the $(5b_1)^{-1}$ and $(11a_1)^{-1}$ ionizations slightly, with a larger increase in VIE being obtained for the $(4b_2)^{-1}$ ionization. The Davidson correction, *Q*, introduces a slight reduction in the VIEs to the X^2B_1 and A^2A_1 ionic states and a slight increase in VIE to the C^2B_2 ionic state. A similar rise is also observed in the $(1b_{2u})^{-1}$ ionization of diborane, an effect large enough to reverse the $^2B_{3u}$ and $^2B_{2u}$ ionic states and restore them to their original KT ordering. Therefore, in the absence of a full set of ΔSCF + CISD (+*Q*) calculations for $GaBH_6$, it is reasonable to assume that the ionic state ordering is the one predicted by both Koopmans' theorem and the DFT results.

Attention is now directed to the fifth band arising from ionization of the $10a_1$ orbital. This orbital arises primarily from bonding interactions of Ga 4s and B 2s atomic orbitals with the 1s orbitals of their respective terminal H atoms; negligible overlap exists between either Ga 4s or B 2s orbitals and the bridging H 1s orbitals. The form of this orbital suggests the vibration most likely to be excited on ionization is the totally symmetric stretching mode of the M−H_t bonds (M = B, Ga). The B−H_t and Ga−H_t symmetric stretching modes of the neutral molecule have vibrational constants of 2482 and 1982 cm^{-1}, respectively.[34,35] Inspection of Figure 2b reveals that two vibrational progressions are present with values for $\bar{\omega}_e$ of 1950 ± 100 and 1480 ± 100 cm^{-1} assigned to the B−H_t and Ga−H_t symmetric stretching modes, respectively, in the D^2A_1 ionic state.

The band associated with the $(9a_1)^{-1}$ ionization was not observed in the He I photoelectron spectrum of $GaBH_6$. Assuming the true VIE of this band lies somewhere between the computed KT and DFT values, then this band must be situated at approximately 20 eV. The intensity of this feature is presumed to be too low to allow detection.

(iii) Ga_2H_6. Comparing the He I photoelectron spectra of diborane (Figure 1), gallaborane (Figure 4), and digallane (Figure 5) reveals a continuation of the trend noted above: the overall spectral envelopes are similar but further shifted to lower energy. Thus, the VIE of the first band is approximately 0.5

eV lower for Ga_2H_6 than for $GaBH_6$; the separation of the first and fourth band maxima is much smaller for Ga_2H_6 at 1.35 eV; and the fifth band of Ga_2H_6 is a further 0.63 eV lower in energy than the corresponding band of $GaBH_6$. Such behavior is wholly consistent with a second Ga atom replacing the B atom in $GaBH_6$.

The rise in symmetry from C_{2v} to D_{2h} means that there was only one ionic state for which it has proved impossible to compute a VIE at the ΔSCF and higher levels of theory, namely, the E^2A_g state. Comparing the results of Tables 4 and 7, it is seen that the KT VIEs are again too high, whereas the DFT values are too low relative to the experimental values. For both methods of calculation, the computed VIE in closest agreement with the experimental value is the $(4b_{2u})^{-1}$ ionization. Overall, the DFT VIEs appear to come closest to matching the experimental VIEs.

Reordering of the first four ionic states occurs at the ΔSCF level of calculation, as found previously for B_2H_6. However, whereas the ionic state ordering for B_2H_6 reverted to the pattern predicted by KT at the ΔSCF + CISD + *Q* level, this is not the case for Ga_2H_6. On the evidence of the results in Table 4, it seems reasonable to assign the $(4b_{2g})^{-1}$ and $(8b_{1u})^{-1}$ ionizations to the first and fifth photoelectron bands, respectively; the order of the other three ionizations, corresponding to the second, third, and fourth bands, is less easily established. The striking similarity which the He I photoelectron spectrum recorded for digallane bears to those displayed by gallaborane and diborane seems to suggest that the ionic state ordering is the same in Ga_2H_6 as in $GaBH_6$ (once the orbital symmetries had been correlated) and B_2H_6. In addition, the $(1b_{2u})^{-1}$ and $(4b_2)^{-1}$ ionizations in diborane and gallaborane, respectively, are established as being associated with the fourth bands in the relevant photoelectron spectra, with the KT and DFT VIEs for the $B_2H_6^+(C^2B_{2u})$ and $GaBH_6^+(C^2B_2)$ ionic states in good agreement with experiment. The only ionic state of Ga_2H_6 with a computed VIE in good agreement with experiment at the KT and DFT levels is the C^2B_{2u} state. These points lead to the tentative assignment of the ionic state ordering for Ga_2H_6 in line with that predicted by Koopmans' theorem and the DFT calculations.

The vibrational constant derived from the progression observed in the fifth band of the He I photoelectron spectrum of Ga_2H_6 is 1540 ± 40 cm^{-1}. This band arises from ionization from the $8b_{1u}$ orbital, which, as mentioned above, is composed predominantly of a bonding interaction of Ga 4s orbitals with the terminal H 1s orbitals, with no contribution from the bridging H atoms. The vibrational mode most likely to be excited on ionization from this orbital is the totally symmetric Ga−H_t stretching mode; the corresponding mode of the neutral molecule in its ground electronic state has a value for $\bar{\omega}_e$ of 2000 cm^{-1}.[3] The observed reduction in frequency on ionization parallels the behavior observed in the B_2H_6 and $GaBH_6$ photoelectron spectra (see above).

The KT and DFT VIEs indicate the presence of the E^2A_g ionic state in the ionization energy region 17.3−19.3 eV. This ionic state may be the origin of the irreproducible weak feature at *ca*. 18 eV. Because of the poor transmission of the electrostatic analyzer to low kinetic energy electrons, any He I band in this IE region would suffer considerable attenuation of intensity.

The He I photoelectron spectrum of Ga_2D_6 is virtually identical to that of Ga_2H_6 (Figures 5 and 6), apart from the vibrational structure observed in the fifth bands. The subtle difference in vibrational envelopes arises from the change in vibrational constants on deuteriation; the measured $\bar{\omega}_e$ values

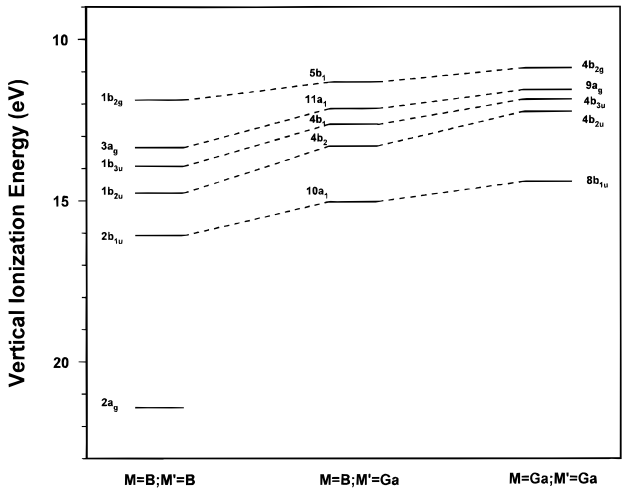

Figure 7. Correlation energy diagram for the valence orbitals of B_2H_6, $GaBH_6$, and Ga_2H_6 derived from the VIEs measured in this work. Ordinate: vertical ionization energy/eV.

are 1540 ± 40 cm^{-1} for $Ga_2H_6^+(D^2B_{1u})$ and 1140 ± 40 cm^{-1} for $Ga_2D_6^+(D^2B_{1u})$. Recently, measurements of the Raman spectra of the matrix-isolated molecules Ga_2H_6 and Ga_2D_6 have identified ν_1, the totally symmetric Ga−X_t stretching fundamentals (X = H, D); the ratio $\bar{\omega}_e(H)/\bar{\omega}_e(D)$ for the neutral molecules is found to be 1.39.[3] For the molecular ions $Ga_2H_6^+$ and $Ga_2D_6^+$, the corresponding $\bar{\omega}_e$ ratio is 1.35 ± 0.07, on the basis of the values derived in this work, consistent with the ratio observed for the neutral molecules.

As a final point of interest, it is valuable to construct a correlation energy diagram for the experimental VIEs from the valence orbitals of the group 13 hydride molecules, $H_2M(\mu\text{-}H)_2M'H_2$ (M, M′ = B or Ga). Such a diagram, displayed in Figure 7, summarizes the main points made above. The valence orbital and ionic state ordering remain consistent, allowing for changes in molecular symmetry on substituting one, and then both, B atoms for Ga in the $H_2B(\mu\text{-}H)_2BH_2$ molecule, with an associated downward trend in VIE.

Conclusions

The valence ionization energies of $GaBH_6$ and Ga_2H_6 have been measured for the first time in this PES study. The He I photoelectron spectra of these molecules are very similar, and a definite correlation in the valence ionization energies of the compounds B_2H_6, $GaBH_6$, and Ga_2H_6 has been observed. For each molecule the valence orbital ordering computed with a reasonably large basis set can be used to give the ionic state ordering. The good agreement between the computed and measured vertical ionization energies of digallane supports a bridge-bonded model, which is well-established for diborane.

Attempts in this work to obtain the He II photoelectron spectra of $GaBH_6$ and Ga_2H_6 were unsuccessful due to the very low intensity of the recorded spectra, although the He II photoelectron spectrum of B_2H_6 was successfully recorded.

For each molecule, the fifth photoelectron band showed resolved vibrational structure which was assigned to a terminal $-BH_2$ or $-GaH_2$ vibration in the ion, on the basis of the atomic orbital characteristics of the orbital from which ionization occurred.

Finally it is hoped that progress in the preparative chemistry of the group 13 hydrides continues so that it will soon be possible to record the UV photoelectron spectrum of Al_2H_6 and compare it to the spectra successfully recorded for B_2H_6 and Ga_2H_6.

Acknowledgment. The authors thank the EC and EPSRC for financial support, which included an EPSRC research studentship (for P.F.S.). L.A. was a Sesquicentennial Associate of the University of Virginia and a Senior Fulbright Scholar while being a Senior Academic Visitor at the University of Oxford.

References and Notes

(1) Downs, A. J.; Goode, M. J.; Pulham, C. R. *J. Am. Chem. Soc.* **1989**, *111*, 1936.
(2) Pulham, C. R.; Downs, A. J.; Goode, M. J.; Rankin, D. W. H.; Robertson, H. E. *J. Am. Chem. Soc.* **1991**, *113*, 5149.
(3) Souter, P. F.; Andrews, L.; Downs, A. J.; Greene, T. M.; Ma, B.; Schaefer, H. F. *J. Phys. Chem.* **1994**, *98*, 12824.
(4) Downs, A. J.; Pulham, C. R. *Adv. Inorg. Chem.* **1994**, *41*, 171.
(5) Downs, A. J.; Pulham, C. R. *Chem. Soc. Rev.* **1994**, *23*, 175.
(6) Lammertsma, K.; Leszczyński, J. *J. Phys. Chem.* **1990**, *94*, 2806.
(7) Duke, B. J. *J. Mol. Struct.* (*THEOCHEM*) **1990**, *208*, 197.
(8) Liang, C.; Davy, R. D.; Schaefer, H. F. *Chem. Phys. Lett.* **1989**, *159*, 393.
(9) Bock, C. W.; Trachtman, M.; Murphy, C.; Muschert, B.; Mains, G. J. *J. Phys. Chem.* **1991**, *95*, 2339.
(10) Trinquier, G.; Malrieu, J. P. *J. Am. Chem. Soc.* **1991**, *113*, 8634.
(11) Duke, B. J.; Liang, C.; Schaefer, H. F. *J. Am. Chem. Soc.* **1991**, *113*, 2884.
(12) Shen, M.; Schaefer, H. F. *J. Chem. Phys.* **1992**, *96*, 2868.
(13) Barone, V.; Orlandini, L.; Adamo, C. *J. Phys. Chem.* **1994**, *98*, 13185.
(14) Breisacher, P.; Siegel, B. *J. Am. Chem. Soc.* **1965**, *87*, 4255. Hara, M.; Domen, K.; Onishi, T.; Nozoye, H. *J. Phys. Chem.* **1991**, *95*, 6.
(15) Barone, V.; Adamo, C.; Fliszár, S.; Russo, N. *Chem. Phys. Lett.* **1994**, *222*, 597.
(16) Stanton, J. F.; Bartlett, R. J.; Lipscomb, W. N. *Chem. Phys. Lett.* **1987**, *138*, 525.
(17) Horn, H.; Ahlrichs, R.; Kölmel, C. *Chem. Phys. Lett.* **1988**, *150*, 263.
(18) Sana, M.; Leroy, G.; Henriet, C. *J. Mol. Struct.* **1989**, *187*, 233.
(19) Rendell, A. P.; T. J. Lee.; Komornicki, A. *Chem. Phys. Lett.* **1991**, *178*, 462.
(20) Price, W. C. *J. Chem. Phys.* **1947**, *15*, 614; **1948**, *16*, 894.
(21) Hedburg, K.; Schomaker, V. *J. Am. Chem. Soc.* **1951**, *73*, 1482.
(22) Bartell, L. S.; Carroll, B. L. *J. Chem. Phys.* **1965**, *42*, 1135.
(23) Kuchitsu, K. *J. Chem. Phys.* **1968**, *49*, 4456.
(24) Rose, T.; Frey, R.; Brehm, B. *J. Chem. Soc., Chem. Commun.* **1969**, 1518.
(25) Lloyd, D. R.; Lynaugh, N. *Philos. Trans. R. Soc. London A* **1970**, *268*, 97.
(26) Brundle, C. R.; Robin, M. B.; Basch, H.; Pinsky, M.; Bond, A. *J. Am. Chem. Soc.* **1970**, *92*, 3863.
(27) Asbrink, L.; Svensson, A.; Von Niessen, W.; Bieri, G. *J. Electron Spectrosc. Relat. Phenom.* **1981**, *24*, 293.
(28) Jones, D. S.; Lipscomb, W. N. *J. Chem. Phys.* **1969**, *51*, 3133.
(29) Jones, D. S.; Lipscomb, W. N. *Acta. Crystallogr. A* **1970**, *26*, 196.
(30) Duncan, J. L.; Harper, J. *Mol. Phys.* **1984**, *51*, 371.
(31) Duncan, J. L. *J. Mol. Spectrosc.* **1985**, *113*, 63.
(32) *Advances in Boron and the Boranes*; Liebmann, J. F., Greenberg, A., Williams, R. E., Eds.; VCH: Weinheim, Germany, 1988.
(33) *Gmelin Handbook of Inorganic Chemistry*, 8th ed.; Boron Compounds, System No. 13, Parts 14, 18, and 20, 2nd and 3rd Supplements, Vol. 1; Springer: Berlin, 1977−1987.
(34) Pulham, C. R. Ph.D. Thesis, University of Oxford, 1991.
(35) Pulham, C. R.; Brain, P. T.; Downs, A. J.; Rankin, D. W. H.; Robertson, H. E. *J. Chem. Soc., Chem. Commun.* **1990**, 177.
(36) Barone, V.; Minichino, C.; Lelj, F.; Russo, N. *J. Comput. Chem.* **1988**, *9*, 518.
(37) van der Woerd, M. J.; Lammertsma, K.; Duke, B. J.; Schaefer, H. F., III. *J. Chem. Phys.* **1991**, 1160.
(38) Dyke, J. M.; Jonathan, N.; Morris, A. In *Electron Spectroscopy*; Brundle, C. R., Baker, A. D., Eds.; Academic Press: New York, 1979; Vol. 3.
(39) Dyke, J. M.; Jonathan, N.; Morris, A. *Int. Rev. Phys. Chem.* **1982**, *2*, 3.
(40) Bulgin, D.; Dyke, J. M.; Goodfellow, F.; Jonathan, N.; Lee, E.; Morris, A. *J. Electron Spectrosc. Relat. Phenom.* **1977**, *12*, 67.
(41) Weiss, H. G.; Shapiro, I. *J. Am. Chem. Soc.* **1959**, *81*, 6167.
(42) Huzinaga, S. *J. Chem. Phys.* **1965**, *42*, 1293.
(43) Dunning, T. H. *J. Chem. Phys.* **1970**, *53*, 2823.
(44) Roos, B.; Siegbahn, P. *Theor. Chim. Acta* **1970**, *17*, 199.
(45) Dunning, T. H. *J. Chem. Phys.* **1977**, *66*, 1382.
(46) Schaefer, H. F.; Ma, B. Private communication.
(47) Amos, R. D. CADPAC: The Cambridge Analytic Derivatives Package, Issue 5.0, Cambridge, 1992.
(48) Koopmans, T. *Physica* **1933**, *1*, 104.
(49) Langhoff, S. R.; Davidson, E. R. *Int. J. Quantum Chem.* **1974**, *8*, 61.
(50) Guest, M. F. *GAMESS User's Guide and Reference Manual*; SERC Daresbury Laboratory: Daresbury, U.K., 1989.
(51) *ADF User's Guide*; Version 1.02, Department of Theoretical Chemistry, Free University: Amsterdam, 1993.
(52) Vosko, S. H.; Wilk, L.; Nusair, M. *Can. J. Phys.* **1980**, *58*, 1200.
(53) Yeh, J. J.; Lindau, I. *At. Data Nucl. Data Tables* **1985**, *32*, 1.
(54) *Chemistry of Aluminium, Gallium, Indium, and Thallium*, Downs, A. J., Ed.; Blackie: Glasgow, Scotland, 1993; pp 2−3.

JP953039C